Effects of triangular gold nanoparticles in the clams *Ruditapes decussatus*

Abdelhafidh Khazri [c*], Badreddine Sellami [a], Amine Mezni [b], Mouhamed Dellali [c], Wiem Saidani [c], Imen Bouzidi [c], David Sheehan [d], Ezzeddine mahmoudi [c], Hamouda Beyrem [c]

[a] *National Institute of Marine Sciences and Technologies, Tabarka, Tunisia*

[b] *Unit of Research 99/UR12-30, Department of Chemistry, Faculty of Sciences of Bizerte, 7021 Jarzouna, Tunisia Department of Chemistry and Faculty of Science, Taif University, Taif, Saudi Arabia*

[c] *Laboratoire de Biosurveillance de l'Environnement (LBE), Unité d'Ecotoxicologie et d'Ecologie Côtière (GREEC), Faculté des Sciences de Bizerte, 7021 Zarzouna–Bizerte, Tunisia*

[d] *Environmental Research Institute and Department of Biochemistry, University College Cork, Western Gateway Building, Western Rd, Cork, Ireland and Khalifa University of Science and Technology, PO Box 127788, Abu Dhabi, United Arab Emirates.*

* Corresponding Author: Abdelhafidh khazri

E-mail address: khazri27@gmail.com

Phone: + 216 50 227 538

Unité d'Ecotoxicologie et d'Ecologie Côtière (GREEC), Faculté des Sciences de Bizerte, 7021 Zarzouna–Bizerte.

Abstract

Context: Many reports link nanoparticles with adverse environmental effects. However, relatively little information is available on how these compounds interact with marine organisms.

Objective: Our aim was to examine the effects of triangular gold nanoparticles (Tr-Au NPs) in the clam, *Ruditapes decussatus*.

Materials and methods: Clams were exposed to Tr-Au1 = 5 µg/L and Tr-Au2 = 10 µg/L for 2 and 7 days to study effects of these nanoparticles. Effects on shell structure were investigated. Superoxide dismutase (SOD), catalase (CAT), glutathione transferase (GST) activities, protein carbonyl levels and malondialdehyde content were used to assess biochemical status.

Results: Transmission electron microscopy and electron dispersive X-ray microanalysis (EDX) showed that gold leads to modification of shell structure and morphology. Indeed, Tr-Au NPs size were altered forming aggregate particles. Triangular gold NPs increased SOD, CAT and GST activities in gill and digestive gland in a concentration- and time-dependent manner indicating defense against oxidative stress. Lipid peroxidation and protein carbonyl levels indicated that Tr-Au NPs caused significant cellular damage.

Conclusion: This study provides a framework for understanding of toxicological effects of nanoparticles on a filter feeding organism. It explores also novel interactions between Tr-Au NPs and bivalve species.

Keywords: Nanoparticles; *Ruditapes decussatus;* Oxidative stress; Biomarkers; Biomonitoring

Introduction

Environmental pollutants, such as nanoparticles (NPs) increasingly used in consumer products and human activities, can be released into marine ecosystems where they may interact with aquatic organisms and induce toxic effects at different levels of biological organization (Li et al. 2013; Maurer-Jones et al. 2013; Baker et al. 2014; Corsi et al. 2014; Minetto et al. 2014; Cid et al. 2015; Grillo et al. 2015). Indeed, NPs can penetrate biobarriers and move easily into and through organisms which can cause toxic effects (Nowack et al. 2007). Oxidative stress histological and morphological changes are often associated with NP toxicity (Li et al. 2013; Cid et al. 2015).

Gold NPs (Au NPs) are used in the medical sector as a contrast agent (Azzay and Mansour, 2009) and in drug delivery systems (Yih and Al-Fandi, 2006). Au NPs are generally regarded as being non-toxic, inert and biocompatible. However, they have also been shown to have some biological effects on the nanoscale (Clough, 2009). Because of their extensive use, Au NPs could potentially represent a significant novel anthropogenic input to the aquatic environment (Lapresta Fernández et al. 2012).

Bivalves are considered prime candidates for uptake of pollutants during environmental contamination scenarios (Galloway et al. 2002; Livingstone, 2001). NP ecotoxicity has been reported in several sentinel species including *Mytilus edulis*, *Ruditapes philippinarum* and *Daphnia magna* (Tedesco et al. 2010; Khan et al. 2014; García Negrete et al. 2015). The Mediterranean clam *Ruditapes decussatus* has been used as a sentinel species in aquatic toxicology due to its tolerance for chemical contaminants (Dellali et al. 2001; Sellami et al. 2015). These organisms are abundant and farmed commercially around the Mediterranean Sea (Mohamed et al. 2003). They are relatively resistant to a wide variety of pollutants and environmental stressors, making them especially suitable in marine biomonitoring. They filter large volumes of pollutants and may represent a significant target for NPs in the aquatic environment (Canesi et al. 2012).

Oxidative stress is recognized as one of the most common effects of nanotoxicity (Klaine et al. 2008). Au NPs are able to induce reactive oxygen species (ROS) production in bivalves triggering oxidative stress. In redox homeostasis, ROS are detoxified by antioxidant defenses which include antioxidant enzymes such as superoxide dismutase (SOD), catalase (CAT) and glutathione transferase (GST). These protect important cellular components such as lipids, proteins, and DNA from oxidative damage. Thus, antioxidant enzyme activity levels can provide valuable information regarding the effects of NPs on an organism's biology (Cid et al. 2015). In addition, shells of bivalve's offer important practical advantages for monitoring

chemical contamination of the aquatic environment (Cravo et al. 2004; Yang et al. 2011; Sellami et al. 2015).

Despite the links between NP exposure and adverse environmental effects in sentinel species such as clams, relatively little information is available on how these compounds might interact with bivalve shells. The present study aims, for the first time, to establish if there is a correlation between activities of antioxidant enzymes and triangular gold NP (Tr-Au NPs) - associated effects on shells of *R. decussatus*.

Materials and methods

Tr-Au NPs Preparation

Tr-Au NPs were produced by a modified polyol process involving a surface regulating polymer, polyvinylpyrrolidone (PVP). Briefly, 25 mL of triethylene glycol (ACROS Organics, 98%) solution, containing 0.038 mMol of hydrogen tetrachloroaurate (III) trihydrate ($HAuCl_4 \cdot 3H2O$) (Sigma-Aldrich), and 0.05 molar ratio of PVP (K30; Sigma-Aldrich) to $HAuCl_4$ were mixed and heated to 150°C. The mixture was held at the same temperature for 30 min under constant agitation. The final colloidal solution had a blue color. The product was separated by centrifugation, washed several times with ethanol/acetone (2:1), and dispersed in MilliQ-water. From this solution, dilutions were prepared directly without allowing the colloid to age. In order to investigate effects of Tr-Au NPs on *R. decussatus*, many Tr-Au NPs suspensions with different concentrations were prepared. For a low-level concentration, the 280 mg L^{-1}Tr-Au NPs suspension was diluted to a 5 µg L^{-1} concentration in standard sea water (SW), and in MilliQ-water, for comparison purposes. For a high-level concentration, the 280 mg L^{-1} Tr-Au NPs suspension was diluted to 10 µg L^{-1}, again in both standard SW and MilliQ-water, according to the required concentration in each particular case throughout this study.

Characterization

Tr-Au NPs characteristics were studied using transmission electron microscopy (TEM) in a JEOL-JFC 1600 microscope operating at 200 keV and an energy-dispersive X-ray spectrograph (EDX). Selected area electron diffraction patterns (SAED) were also acquired in order to determine the crystallographic orientation of NP facets. The optical absorption spectra of diluted Tr-Au NPs solution were performed on a Perkin-Elmer Lambda 11 UV/VIS spectrophotometer.

Animals and treatments

Adult clams (*R. decussatus*) of 2.5-3 cm shell length (maximum axis) were obtained from a site in Bizerte lagoon (37°13'18.54''N, 9°55'59.61''E). Acclimation occurred in free-flow tanks for one week before commencing exposures. For the course of the experiment, 5 individuals were placed in each tank with 3 L of SW obtained from the sampling site (salinity 37, temperature 18°C, oxygen at 6.5 mg/L), containing 5 and 10 µg/L of Tr-Au NPs respectively. A control series without Tr-Au NPs was run in parallel. Each experiment was performed in triplicate. Exposure treatments are denoted as follows: Tr-Au1 for 5 µg/L gold concentration and Tr-Au2 for 10 µg/L gold concentration. The concentrations selected, while higher than environmental levels, were chosen on the basis of previous results considered for Au NP effects on bivalves and because they have previously shown mild oxidative stress responses (Tedesco et al. 2008, 2010). Aeration at the bottom of the tank was used to minimize agglomeration and subsequent sedimentation of the contaminant, and SW was changed every 48 h. For the duration of the experiment (2 and 7 days), Tanks were filled with natural SW changed every 48 h and the environmental parameters were the same as those used for the acclimation period. Test animals were checked daily. No mortality was observed and all animals were seen to be feeding normally. Unexposed and Tr-Au NP-exposed clams were collected after 2 and 7 days. Animals were dissected. Gill and digestive gland were collected, immediately frozen in liquid nitrogen and stored at -80 °C until required. Shells of control and treated clams were retained after 2 and 7 days, dried, crushed manually to obtain a powder with grain size of 80-200 µm and stored at 4°C prior to chemical characterization.

Biochemical analysis

Digestive gland and gill were homogenised by a polytron homogenizer in 10 mM Tris/HCl, pH 7.2, containing 500 mM sucrose, 1mM EDTA and 1 mM PMSF, supernatants were collected by centrifugation at 20,000 × g (4°C for 30 min). Antioxidant enzymatic activities were measured in the cytosolic fraction of 15 clams from controls and groups exposed to Tr-Au NPs. Changes in optical density were quantified using a Beckman DU500 spectrophotometer. Protein content was estimated by the method of Bradford (1976) using bovine serum albumin (BSA) as a standard. SOD activity was assessed by the ability of the enzyme to inhibit auto-oxidation of pyrogallol. We used 0.2 mM pyrogallol in air-equilibrated

50 mM Tris- buffer pH 8.20, containing 1 Mm EDTA (Marklund and Marklund, 1974) and is expressed in µmol/min/mg of total protein. CAT activity was measured by the decrease in absorbance at 240 nm due to H_2O_2 consumption (Aebi,1974). The reaction volume and reaction time were 1 mL and 1 min, respectively. The reaction solution contained 80 mM phosphate buffer, pH 6.5 and 50 mM H_2O_2 (Ni et al., 1990) and CAT activity is given as nmol/min/mg protein. GST activity was measured by a modification of the method of Habig et al.1974. There action mixture contained 200 µL supernatant, 2mLphosphate buffer (0.125 M, pH 7.7,containing Na_2 EDTA ,0.05 M, 2–4 °C), H_2O 400 µL, 200 µL 15mM 1-chloro-2,4-dinitrobenzene (CDNB) dissolved in 95% ethanol and 200 µL 15mM of reduced glutathione (GSH).GST activity was determined following the conjugation of GSH with CDNB at 340 nm. A unit of GST activity was defined as the amount of glutathione conjugate formed using 1nM GSH and CDNB/min per mg protein (nM 2,4-dinitrophenyl glutathione/mg protein/min).

Lipid peroxidation was determined in terms of thiobarbituric acid reactive species (TBARS), by malondialdehyde (MDA; Buege and Aust, 1978). Briefly, 1mL sample extract was mixed with 2mL of trichloroacetic acid-thiobarbituric acid-HCl (TCA–TBA–HCl) reagent (15% (w/v) TCA, 0.375% (w/v) TBA and 0.25 N HCl). Mixture was boiled for 15 min, cooled and centrifuged at 10,000g to remove precipitate. Absorbance was measured at 535 nm and MDA content was calculated using an extinction coefficient of 156 mM^{-1} cm^{-1}. Lipid peroxidation was expressed as nMol MDA/mg protein.

Protein carbonyl levels were also determined (Levine et al., 1990). After incubation, the assay mixture was centrifuged at 10,000g for 10 min at 4 °C and the supernatant precipitated with TCA followed by centrifugation at 10,000g for 3 min. The pellet was resuspended in 2, 4-dini-trophenyl hydrazine and incubated at 25 °C for 60 min. Proteins were then precipitated with TCA. The mixture was then centrifuged and the pellet was washed with acetone three times. Absorbance was measured at 360 nm and carbonyl content was calculated using a molar extinction coefficient of 22 mM^{-1} cm^{-1}. Results were expressed as nMol carbonyl/mg protein.

Statistical analyses

Statistical analysis was performed using STATISTICA 8.0. Results of enzymatic activities were reported as mean ± standard deviation. Variation of each enzyme across time and concentration was tested by one-way ANOVA ($p < 0.05$). Previously, we tested the pre-requisites for analysis of variance (normality and homogeneity of variances). When significant differences were found, Tukey's test was applied to determine which values differed significantly.

Results

Morphological and elemental analysis

A representative TEM image of the synthesized NPs is shown in Fig. 1a. The majority of NPs were equilateral triangular prisms with an average edge length of 150 nm (Fig. 1b). Energy dispersive spectrum (EDX) analysis for the sample confirmed that Tr-Au NPs consist of only gold (Fig. 1c, the copper element originated from copper grid). An inset to Fig.1a, gives typical selected area electron diffraction (SAED) pattern obtained by directing the electron beam perpendicular to a single gold nanoplate deposited flat on the TEM grid. The hexagonal symmetrical spots of the SAED pattern show that gold nanoplates are single crystals and the incident electron beam is perpendicular to the {111} facet of the tested plate. The absorbance spectrum of the as-prepared colloidal solution (Fig.1.D) show an extinction band with a maximum intensity around 720 nm due to the contribution of in-plane dipole SPR absorption of anisotropic products in which the oscillation of free electrons was strongly restricted in the planar structure. Structural characterization of shell and the nanosize distribution of unexposed and Tr-Au exposed clams determined by TEM and EDX are depicted in Fig 2. The detailed structure of the pure shell is seen in Fig 2. (a,b) while TEM images show an alternation of homogeneous light and dark layers with an average length of 1µm as indicated by the scale bar of 300 nm.

Shell structure seems to resemble a complex cross-lamellar structure. This is in good agreement of the findings of Yang et al. (2011). Indeed, the different $CaCO_3$ polymorphs can form diverse types of structure, such as prismatic, sheet nacreous, lenticular nacreous, foliated, cross-lamellar, complex cross lamellar and homogeneous structure (Taylor and Layman, 1972; Currey and Taylor, 1974). The EDX spectrum confirms the components and the purity of the shell which is composed essentially of calcium carbonate ($CaCO_3$), in general about 95 wt.% and less than 5 wt.% organic materials (Currey., 1977). The two principal polymorphs of $CaCO_3$ in shells are aragonite and calcite (Sellami et al. 2015). Figure 2-d, shows the influence of Tr-

Au NPs exposure on the structure and morphology of the shell. The EDX spectrum (Fig 2-e) confirms the presence of Au NPs (Au element is detected) in the shell after exposure. The Ca and O elements refer to the aragonite composition of the shell. The presence of Cu is due to the copper grid used for the TEM/EDX experiments. As shown in Fig 2-d, and compared to the TEM images of pure clam shell (Fig.2-a) and pure Tr-Au NPs (Figure 1a), the size of gold and clam shell were changed. Indeed, the size of pure Tr-Au NPs as shown in Figure 1-a, is in the range of 150 nm however it was approximately 300 nm (Fig.2-d) after exposure. The same phenomenon was observed for the shell itself; the size was changed from ~1 µm in unexposed clams (Fig.2-d) to a few nanometers (100 - 400 nm) in the Tr-Au2 NPs-exposed animals. To explain this phenomenon, it should be noted that clam shel are porous structures (Yang et al. 2011). Indeed, based on the work of Yang et al. (2011), the pore size can range from 300 to 500 nm. On the other hand, it was previously found that Au NPs can bioaccumulate in clams, forming aggregate particles (Pan et al. 2012). Consequently, it is likely that the size increase from 150 (pure Tr-Au NPs) to 300 nm (in the Tr-Au NPs exposed clams) on bioaccumulation of Tr-Au NPs through clam shell pores leads to modification of the shell structure when the pores become saturated. This can explain also the behavior of the clam shell observed in Fig.2-d and the Tr-Au NPs -induced alteration of size from ~1µm to the nanometer scale (~ 100 to 300 nm). These results are very important in understanding the reactivity of NPs with clams in environmental contexts. García-Negrete et al. (2013) showed that agglomerates can be formed for Au NPs in artificial SW and this result is related to NP concentration in the SW medium.

Biomarker responses to Tr-Au NPs exposure

SOD, CAT and GST activities of clams treated with Tr-Au1 and Tr-Au2 NPs for 2 and 7 days, respectively, were determined (Figs. 3 and 4). Tr-Au NPs induced an overall concentration- and time-dependent increase in antioxidant enzyme activity in both gill and digestive gland. SOD activity in digestive gland after 2 days exposure increased by 28% compared to controls with no effect on gill SOD activity after this exposure time. After 7 days of exposure, SOD activity increased in both gill and digestive gland (Fig. 4). A different pattern of variation in CAT activity was observed between gills and digestive gland after 48 h exposure (Fig.3). Indeed, 2 days of exposure did not alter CAT activity in gills. In contrast, digestive gland CAT activity increased in groups treated with Tr-Au1 and Tr-Au2, respectively. Exposure to Tr-Au1 and Tr-Au2 for 7 days caused a significant ($p < 0.05$) increase of CAT activity in both tissues (Fig. 4). CAT activity increased by approximately 30% and 42% in gill of treated

groups exposed respectively to Tr-Au1 and Tr-Au2 and by about 18% and 47% in digestive gland. The pronounced effect of Tr-Au NPs in gill was supported by morphological changes visible after 7 days of exposure. Gill GST activity increased from 0.74 ± 0.1 nmol/min/mg protein to 1.26 ± 0.28 nmol/min/mg protein in Tr-Au1-treated groups and to 1.33 ± 0.42 nmol/min/mg protein in Tr-Au2-treated groups ($p = 0.045$; $p = 0.023$). Digestive gland GST activity increased in a concentration-dependent manner by approximately 9% and 20%, respectively, on exposure to Tr-Au1 and Tr-Au2. Lipid peroxidation determined by measuring MDA content, and protein carbonyl levels of clams exposed to Tr-Au NPs were similar to the control after 2 days of exposure (Fig. 5). However, after 7 days of exposure, Tr-Au NPs increased protein carbonyl and MDA levels significantly ($p < 0.05$) for both concentrations and in both tissues (Fig. 6).

Discussion

Ecotoxicological effects of gold nanoparticles have so far not been extensively studied. This study aimed to assess the impact of Tr-Au NPs on key antioxidant biomarkers and to explore potential risks posed by this NP to the sentinel species *R. decussatus*. SOD, CAT and GST are involved in the defense against oxidative stress (Regoli et al. 2011). Induction of these enzyme activities are consistent with production of ROS (reactive oxygen species) in response to Tr-Au NPs exposure since it is known that NPs are capable of crossing cell membranes, leading to cell damage (Li et al. 2010). In addition, the pronounced effect in the digestive gland even of short-term exposure may suggest that Tr-Au NPs may be concentrated in digestive gland rather than gill (Tedesco et al. 2008; García-Negrete et al. 2013). Exposure to Tr-Au2 NPs increased SOD activity after 2 days in both tissues. This result suggests that SOD responds to Tr-Au2 NPs stress effects generated in both tissues after 7 days most likely to protect stressed cells. This finding underlines the importance of exposure time in the biochemical response of *R. decussatus* to NPs. A similar pattern was previously reported in mussels upon exposure to Ag NPs with a significant increase along the exposure period (Gomes et al. 2014).

Our data are also in agreement with a previous study showing that Au NPs cause oxidative stress in bivalves, especially in digestive gland (Tedesco et al. 2008). Presumably, NPs are ingested more efficiently when clams are exposed to Au NPs forming aggregate particles (Pan et al. 2012). NPs are also known to interact with thiol-groups that are found in many antioxidant proteins and which, when oxidized, can result in inhibition/inactivation of enzymes (SOD and CAT) as oxidative stress develops (Bar-Ilan et al. 2009; Lapresta-Fernandez

et al. 2012). Tedesco et al. (2008) showed that Au NPs caused oxidative stress in mussel digestive gland (induction of CAT) but also in gill. On the other hand, GST is known to protect cells against ROS during oxidative processes as part of phase II biotransformation (Livingstone, 2001). GST has already been associated with the metabolism of pollutants in bivalves (Sheehan and Power, 1999) and identified as a metabolic pathway for NP metabolism (Wiegand et al. 2001). Our data also agree well with a previous study showing a significant increase of GST activity in a time- and concentration-dependent manner (Cid et al. 2015).

Malondialdehyde (MDA) and protein carbonyl levels are often altered in NP-induced toxicity (Ma et al. 2010; Tedesco et al. 2010) and they are regarded as predictive biomarkers for oxidative stress (Xu et al. 2011). Our results are in good agreement with Chandurvelan et al. (2013) who found a significant increase in CAT activity in digestive gland of the mussel *Perna canaliculus*, while lipid peroxidation levels remained unchanged. Vale et al. (2014) obtained similar results in the freshwater bivalve *Corbicula fluminea* when studying the effect of TiO_2 NPs on the MDA content after 10 days of exposure. TiO_2 NPs showed significant effects on MDA generation. These authors suggest that the presence of the NPs in the medium contributes to cell damages as confirmed by lipid peroxidation data. Additionally, hydrophobic interactions between proteins and lipids might alter protein conformation, thus affecting enzyme activities. Both lipid peroxidation and increased protein carbonyl levels are biochemical perturbations resulting from oxidative stress (Khazri et al. 2015). Changes in carbonyls were previously reported in *M. edulis* in response to Au NPs-citrate and CuO NPs (Tedesco et al. 2008; Hu et al. 2014). These authors correlated increased protein carbonylation with oxidative stress related to ROS production on exposure to NPs.

Conclusions

The present study contributes new information about the nano-toxicity of Tr-Au NPs in the marine bivalve *R. decussatus*. Several toxicological endpoints were altered by Tr-Au NPs exposure: (i) morphological changes to shells and NPs (ii) significant increases in SOD, CAT and GST activities in digestive gland and gill in concentration- and time-dependent manner and (iii) increased lipid peroxidation and protein carbonyl levels in both organs after 7 days of NP exposure. Exposure to Tr-Au NPs disrupts the oxidant/antioxidant balance in the

organs of *R. decussatus*, leading to induction of oxidative stress and cellular damage. Furthermore, considering the increasing prevalence of nanotechnology, the present study provides valuable information regarding the interaction between NPs and biota suggesting potential risks for mollusks bivalves, notably to their shell structure. Further investigation focusing in more depth on the mechanisms of nanomaterial incorporation and interaction with marine organisms are required. This will help us understand the toxicity of NPs and can be used on the programs of environmental risk assessments.

Acknowledgments

This work was supported by grants from the National Institute of Marine Sciences and Technologies, the Ministry of Higher Education, Carthage (Tunisia), Laboratory of Environment Biomonitoring, Unit of research 99/UR12-30 and Department of Chemistry, Faculty of Sciences of Bizerte 7021 Jarzouna (Tunisia).

Declaration of interest

Authors do not have any potential conflict of interest

Ethical statement

The study complied with the declaration of Helsinki.

References

Aebi, H., 1974. Catalase In: Bergmeyer, H.U. (Ed.), Methods of Enzymatic Analysis. Academic Press, London, pp. 671–684.

Aebi, H., 1984. Catalase *in vitro*. Methods Enzymol 105: 121–126 Azzay HME, Mansour MMH (2009) *In vitro* diagnostic prospects of nanoparticles. Chim Acta. 403, 1-8.

Baker, T.J., Tyler, C.R., Galloway, T.S., 2014. Impacts of metal and metal oxide nanoparticles on marine organisms. Environ. Pollut. 186, 257-271.

Bar-Ilan, O., Albrecht, R.M., Fako, V.E., Furgeson, D.Y., 2009. Toxicity Assessments of Multisized Gold and Silver Nanoparticles in Zebrafish Embryos. Small. 5, 1897-1910.

Bradford, M.M., 1976. A rapid and sensitive method for the quantization of micro-gram quantities of protein utilizing the principle of protein-dry binding. Anal. Biochem. 72, 248–254.

Buege, J.A., Aust, S.D., 1978. Microsomal lipid peroxidation. Methods. Enzymol. 52, 302–310.

Canesi, L., Ciacci, C., Fabbri, R., Marcomini, A., Pojana, G., Gallo, G., 2012. Bivalve molluscs as a unique target group for nanoparticle toxicity. Mar. Environ. Res. 76, 16–21.

Chandurvelan, R., Marsden, I.D., Gaw, S., Glover, C.N., 2013. Biochemical biomarker responses of green-lipped mussel, *Perna canaliculus*, to acute and subchronic waterborne cadmium toxicity. Aquat. Toxicol. 140-141, 303–313.

Cid, A., Picad, A., Correia, J.B., Chaves, R., Silva, H., Caldeira, J., de Matos, A.P.A., Diniz, M.S., 2015. Oxidative stress and histological changes following exposure to diamond nanoparticles in the fresh water Asian clam *Corbicula fluminea* (Müller, 1774). J. Hazardous. Materials. 284, 27–34.

Clough, S.R., 2009. The potential ecological hazard of nanomaterials. In: Sellers, et al. (Eds.), Nanotechnology and the Environment. CRC Press, Boca Raton, Fl. 169-192

Corsi, I., Cherr, G.N., Lenihan, H.S., Labille, J., Hassellov, M., Canesi, L., Dondero, F., Frenzilli, G., Hristozov, D., Puntes, Â.V., Della Torre, C., Pinsino, A., Libralato, G., Marcomini, A., Sabbioni, Â.E., Matranga, V., 2014. Common strategies and technologies for the ecosafety assessment and design of nanomaterials entering the marine environment. ACS Nano. 8, 9694-9709.

Cravo, A., Bebianno, M.J., Foster, P., 2004. Partitioning of trace metals between soft tissues and shells of *Patella aspera*. Environ. Int. 30, 87–98.

Currey, J.D., 1977. Mechanical Properties of Mother of Pearl in Tension. The Royal Society, DOI: 10.1098/rspb.1977.0050.

Currey, J.D., Taylor, J.D., 1974. The mechanical behaviour of some molluscan hard tissues. J Zool. Lond. 173, 395–406.

Daughton, C.G., 2004. Non-regulated water contaminants: emerging research. Environ. Impact. Asses. Rev. 24, 711–32.

Dellali, M., Gnassia-Barelli, M., Romeo, M., Aissa, P., 2001. The use of acetylcholinesterase activity in *Ruditapes decussatus* and *Mytilus galloprovincialis* in the biomonitoring of Bizerta lagoon. Comp. Biochem. Physiol. C. 130, 227–235.

Galloway, T.S., Sanger, R.C., Smith, K.L., Fillmann, G., Readman, J.W., Ford, T.E., et al. 2002. Rapid assessment of marine pollution using multiple biomarkers and chemical immunoassays. Environ. Sci. Technol. 36, 2219–2226.

García-Negrete, C.A., Blasco, J., Volland, M., Rojas, T.C., Hampel, M., Lapresta-Fernández, A., Jiménez de Haro, M.C., Soto, M., Fernández, A., 2013. Behaviour of Au-citrate nanoparticles in seawater and accumulation in bivalves at environmentally relevant concentrations. Environ. Pollut. 174, 134–141.

García-Negrete, C.A., Jiménez de Haro, M.C., Blasco, J., Sotoc, M., Fernández, A., 2015. STEM-inSEM high resolution imaging of gold nanoparticles and bivalve tissues in bioaccumulation experiments. Anal. DOI: 10.1039/c4an01643b

Gomes, T., Pereira, C.G., Cardoso, C., Sousa, V.S., Teixeira, M.R., Pinheiro, J.P., Bebianno, M.J., 2014. Effects of silver nanoparticles exposure in the mussel *Mytilus galloprovincialis*. Mar. Environ. Res. 101, 208–214.

Grillo, R., Rosa, A.H., Fraceto, L.F., 2015. Engineered nanoparticles and organic matter: a review of the state-of-the-art. Chemosphere. 119, 608-619.

Habig, W., Pabst, M.J., Jacobi, W.B., 1974. The first enzymatic step in mercapturic acid formation. J. Biol. Chem. 249, 7130–7139.

Howard, C.V., 2014. Small particles — big problems. Int Lab News. 34, 28–9.

Khan, F.R., Kennaway, G.M., Croteau, M.N., Dybowska, A., Smith, B.D., Nogueira, A.J.A., Rainbow, P.S., Luoma, S.N., Valsami-Jones, E., 2014. *In vivo* retention of ingested Au NPs by *Daphnia magna*: No evidence for trans-epithelial alimentary uptake. Chemosphere. 100, 97–104.

Khazri, A., Sellami, B., Dellali, M., Corcellas, C., Eljarrat, E., Barceló, D., Mahmoud, E., 2015. Acute toxicity of cypermethrin on the freshwater mussel *Unio gibbus*. Ecotoxicology and Environmental Safety. 115, 62–66.

Klaine, S.J., Alvarez, P.J.J., Batley, G.E., Fernandes, T.F., Handy, R.D., Lyon, D.Y., Mahendra, S, McLaughlin, M.J., Lead, J.R., 2008. Nanomaterials in the environment: fate, bioavailability and effects. Environ. Toxicol. Chem. 27, 1825–1851.

Lapresta-Fernández, A., Fernández, A., Blasco, J., 2012. Nanoecotoxicity effects of engineered silver and gold nanoparticles in aquatic organisms. TrAC Trends in Analytical Chemistry. 32, 40–59

Levine, R.L., Garland, D., Oliver, C.N., Amici, A., Climent, I., Lenz, A.G., 1990. Determination of carbonyl content in oxidatively modified proteins. Methods Enzymol. 186, 464–478.

Li, H., Turner, A., Brown, M., 2013. Accumulation of aqueous and nanoparticulate silver by the marine gastropod *Littorina littorea*. Water Air Soil Pollut. 224,1–9.

Li, J., Zhu, Y., Li, W., Zhang, X., Peng, Y., Huang, Q., 2010. Nanodiamonds as intracellular transporters of chemotherapeutic drug. Biomaterials. 31, 8410–8418.

Livingstone, D.R., 2001. Contaminant-stimulated reactive oxygen species production and oxidative damage in aquatic organisms. Mar. Pollut. Bull., 42, 656–666.

435 Marklund, S., Marklund, G., 1974. Involvement of the superoxide anion radical in the
436 autoxidation of pyrogallol and a convenient assay for superoxide dismutase. Eur. J.
437 Biochem. 47, 469–474.
438 Maurer-Jones, M.A., Gunsolus, I.L., Murphy, C.J., Haynes, C.L., (2013) Toxicity of engineered
439 nanoparticles in the environment. Anal. Chem. 85, 3036-3049.
440 Minetto, D., Libralato, G., Volpi Ghirardini, A., 2014. Ecotoxicity of engineered TiO_2
441 nanoparticles to saltwater organisms: an overview. Environ. Int. 66, 18-27.
442 Mohamed, B., Rym, B.D., Amor, E.A., Hamadi, B., 2003. Genotoxicity, catalase, and
443 acetylcholinesterase in the assessment of the pollution status of some sites on the Tunisian
444 littoral. Bull. Environ. Contam. Toxicol. 70, 854–860.
445 Nel, A.E., Madler, L., Velegol, D., Xia, T., Hoek, E.M.V., Somasundaran, P., et al. 2009.
446 Understanding biophysicochemical interactions at the nano-bio interface. Nat. Mater. 8,
447 543–57.
448 Ni, W., Trelease, R.N., Eising, R., 1990. Two temporally synthesized charge subunits interact
449 to form the five isoforms of cottonseed (*Gossypium hirsutum*) catalase. Biochem. 269, 233–
450 238.
451 Nowack, B., Bucheli, T.D., 2007. Occurence, behavior, and effects of nanoparticles in the
452 environment. Environ. Pollut. 150, 5–22.
453 Oberdorster, G., Stone, V., Donaldson, K., 2007. Toxicology of nanoparticles: a historical
454 perspective, Nanotoxicol. 1, 2–25.
455 Pan, J.F., Buffet, P.E., Poirier, L., Triquet, C.A., Gilliland, D., Joubert, Y., Pilet, P., Guibbolini,
456 M., de Faverney, C.R., Roméo, M., Jones, E.V., Mouneyrac, C., 2012. Size dependent
457 bioaccumulation and ecotoxicity of gold nanoparticles in an endobenthic invertebrate: The
458 Tellinid clam *Scrobicularia plana*. Environ. Pollut. 168, 37–43.
459 Regoli, F., Benedetti, M., Giuliani, M.E., 2011. Antioxidant defenses and acquisition of
460 tolerance to chemical stress. In: Amiard-Triquet C, Rainbow PS, Roméo M. (Eds.),
461 Tolerance to Environmental Contaminants. CRC Press, Boca Raton, FL.
462 Sellami, B., Khazri, A., Mezni, A., Louati, H., Dellali, M., Aissa, P., Mahmoudi, E., Beyrem,
463 H., Sheehan, D., 2015. Effect of permethrin, anthracene and mixture exposure on shell
464 components, enzymatic activities and proteins status in the Mediterranean clam *Venerupis*
465 *decussata.* Aquat. Toxicol. 158, 22–32.
466 Sheehan, D., Power, A., 1999. Effects of seasonality on xenobiotic and antioxidant defence
467 mechanisms of bivalve molluscs. Comp. Biochem. Physiol. 123, 193–199.

468 Taylor, J.D., Layman, M., 1972. The mechanical properties of bivalve (Mollusca) shell
469 structures. Palaeontol. 15, 73–87.
470 Tedesco, S., Doyle, H., Blasco, J., Redmond, G., Sheehan, D., 2010. Oxidative stress and
471 toxicity of gold nanoparticles in *Mytilus edulis*. Aquat. Toxicol. 100, 178–196.
472 Tedesco, S., Doyle, H., Redmond, G., Sheehan, D., 2008. Gold nanoparticles and oxidative
473 stress in *Mytilus edulis*. Mar. Environ. Res. 66, 131.
474 Vale, G., Franco, C., Diniz, M.S., dos Santos, M.M.C., Domingos, R.F., 2014. Bioavailability
475 of cadmium and biochemical responses on the freshwater bivalve *Corbicula fluminea* – the
476 role of TiO_2 nanoparticles. Ecotoxicology and Environmental Safety. 109, 161–168.
477 Wiegand, C., Krause, E., Steinberg, C., Pflugmacher, S., 2001. Toxicokinetics of atrazine in
478 embryos of the zebrafish (*Danio rerio*). Ecotoxicol. Environ. Saf. 49, 199–205.
479 Wolff, S.P., 1994. Ferrous ion oxidation in presence of ferric ion indicator xylenol orange for
480 measurement of hydroperoxides. Methods Enzymol. 233, 182–189.
481 Yang, W., Kashani, N., Li, X.W., Zhang, G.P., Meyers, M.A., 2011. Structural characterization
482 and mechanical behavior of a bivalve shell (*Saxidomus purpuratus*). Materials Science and
483 Engineering C 31, 724–729.
484 Yih, T.C., Al-Fandi, M., 2006. Engineered nanoparticles as precise drug delivery systems. J.
485 Cell. Biochem. 97, 1184–1190.
486 Zuykov, M., Pelletier, E., Belzile, C., Demers, S., 2011. Alteration of shell nacre
487 micromorphology in blue mussel *Mytilus edulis* after exposure to free-ionic silver and silver
488 nanoparticles. Chemosphere. 84, 701–706.
489

Figure legends:

Fig. 1. (a) TEM images, (b) particle size distribution, (c) EDX spectrum of triangular gold NPs. (d) Plasmonic response of Tr-Au NPs dispersed in ethanol. The inset in (a) shows typical selected area electron diffraction (SAED) pattern from a single NP.

Fig. 2. TEM images (a, b) and EDX spectrum (c) of pure clam shells (chemical formula; $CaCO_3$), (d, e) TEM image and EDX spectrum of Tr-Au NPs of exposed clams. The inset in (d) shows typical selected area electron diffraction (SAED) pattern from Tr-Au NP-exposed clams.

Fig. 3. SOD, CAT and GST activities after two days exposure. Specific activities in gill and digestive gland of untreated (Control) and treated (Tr-Au1 = 5 µg/L andTr-Au2 = 10 µg/L) *R. decussatus* after 2 days exposure to Tr-Au NPs. Different letters indicate statistical differences ($p < 0.05$) compared to control. Data are mean ± SD.

Fig. 4. SOD, CAT and GST activities after seven days exposure. Specific activities in gill and digestive gland of untreated (Control) and treated (Tr-Au1 = 5 µg/L and Tr-Au2 = 10 µg/L) *R. decussatus* after 7 d of exposure to Tr-Au NPs. Different letters indicate statistical differences ($p < 0.05$) compared to control. Data are mean ± SD.

Fig. 5. Effect of 2 days Tr-Au NPs treatment on MDA and protein carbonyl levels in gill and digestive gland of *R. decussatus*. All values are given as means (n = 5). Groups with different letters are significantly different (ANOVA, post-hoc, Tukey HSD test, STATISTICA 8.0, $p < 0.05$).

Fig. 6. Effect of 7 days Tr-Au NPs treatment on malondialdehyde and protein carbonyls levels in gill and digestive gland of *R. decussatus*. All values are given as means (n = 5). Groups with different letters are significantly different (ANOVA, post-hoc, Tukey HSD test, STATISTICA 8.0, $p < 0.05$).

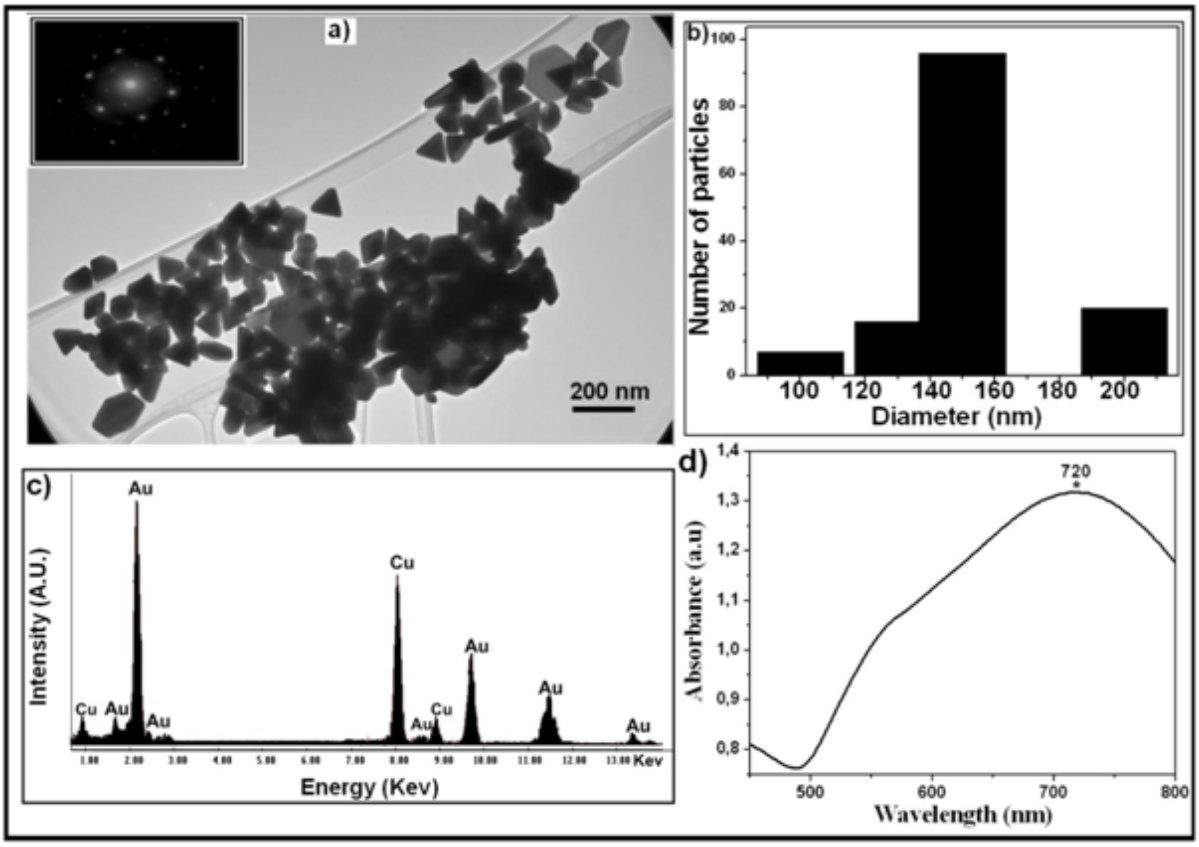
a)
200 nm
b)
Number of particles
Diameter (nm)
c)
Intensity (A.U.)
Au
Cu
Energy (Kev)
d)
720
Absorbance (a.u)
Wavelength (nm)

Fig. 1

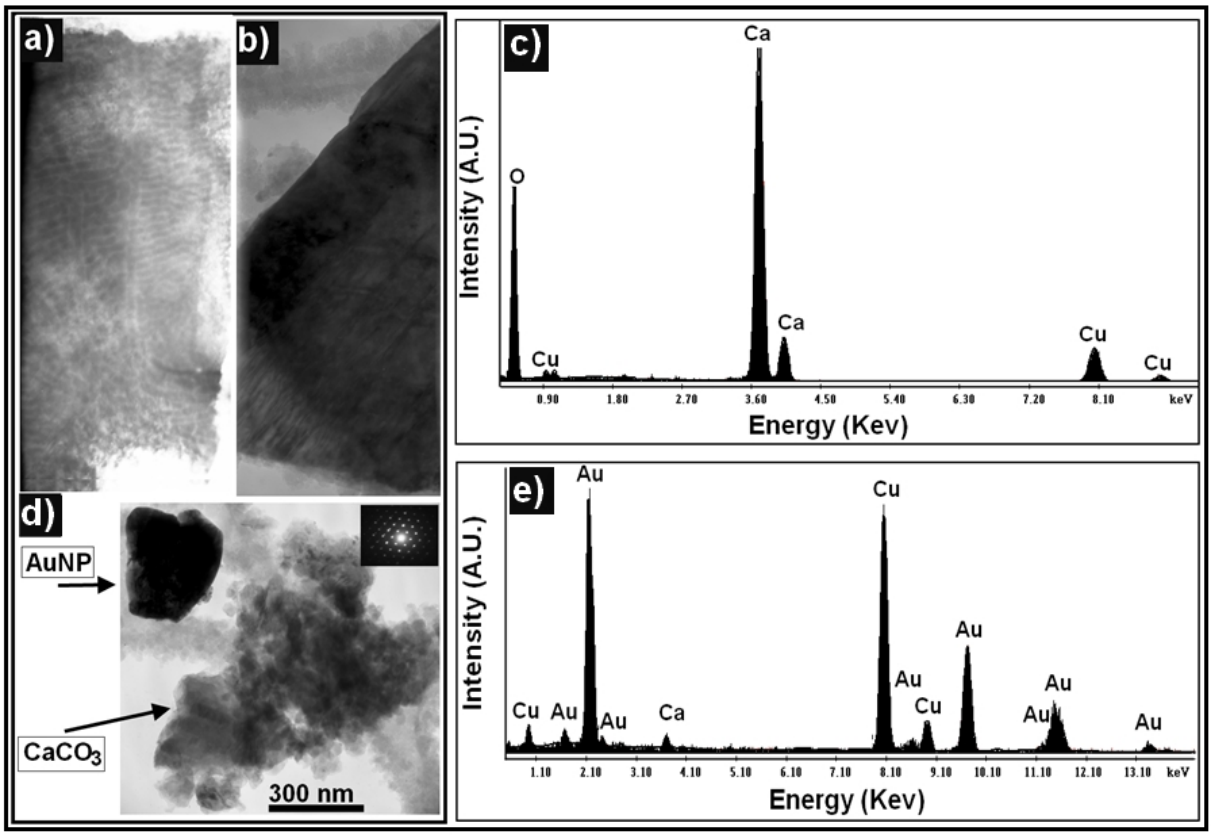
a)
b)
c)
Ca
O
Cu
Ca
Cu
Cu
Intensity (A.U.)
0.90 1.80 2.70 3.60 4.50 5.40 6.30 7.20 8.10 keV
Energy (Kev)
d)
AuNP
CaCO3
300 nm
e)
Au
Cu
Au
Cu Au Au Ca
Au
Cu
Au
Au
Au
Intensity (A.U.)
1.10 2.10 3.10 4.10 5.10 6.10 7.10 8.10 9.10 10.10 11.10 12.10 13.10 keV
Energy (Kev)

Fig. 2

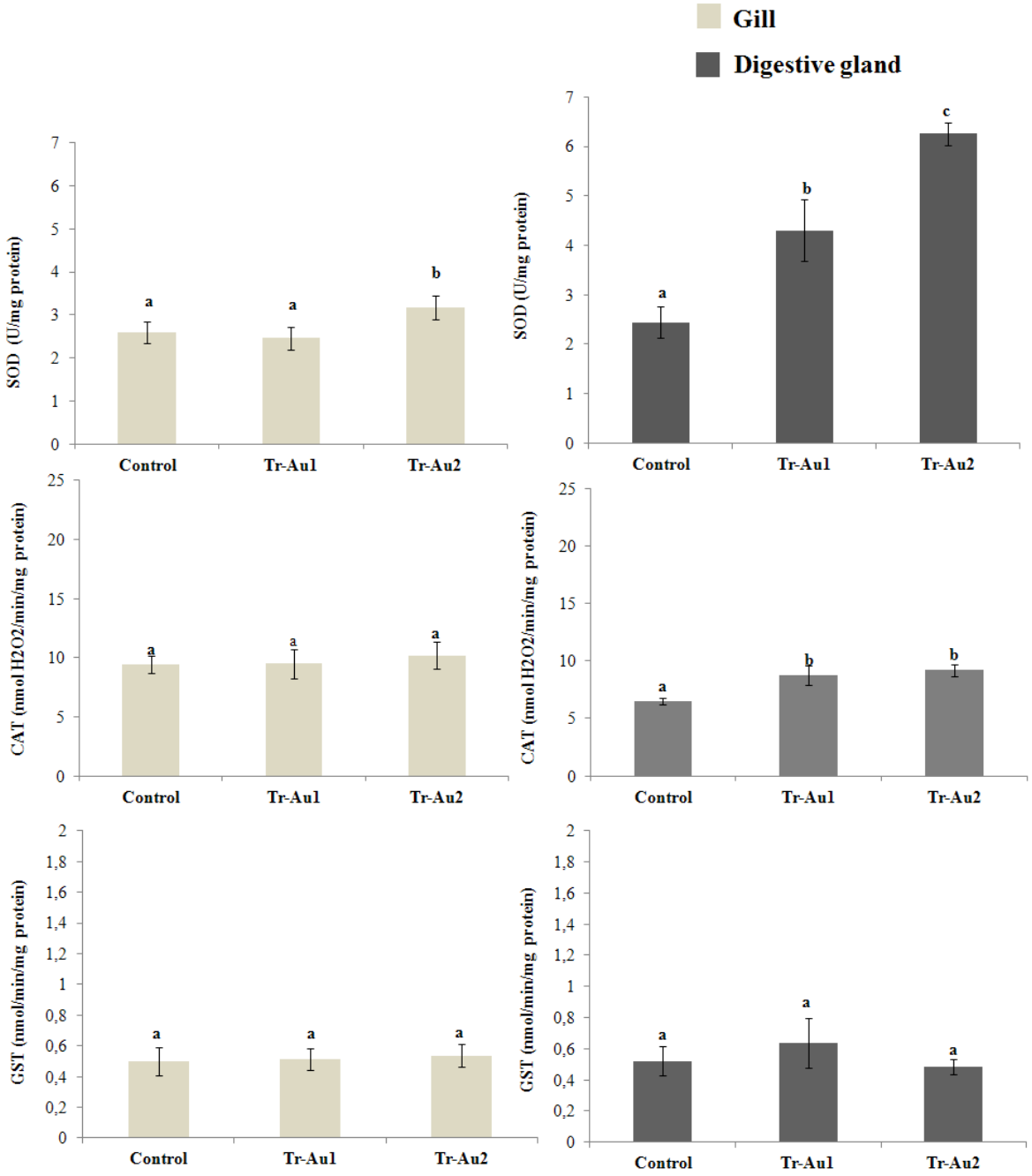

524

525 Fig. 3

526

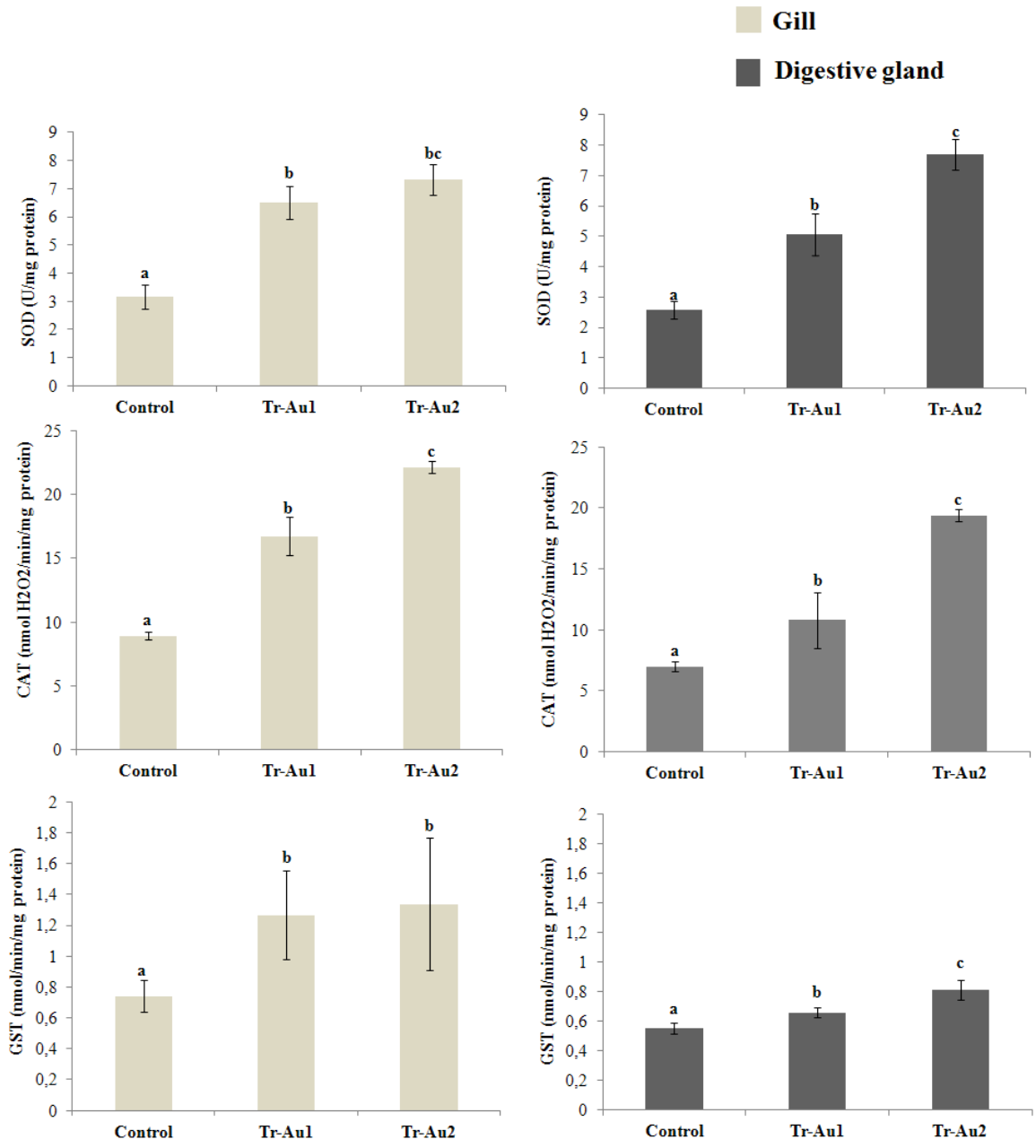

527

528 Fig. 4

529

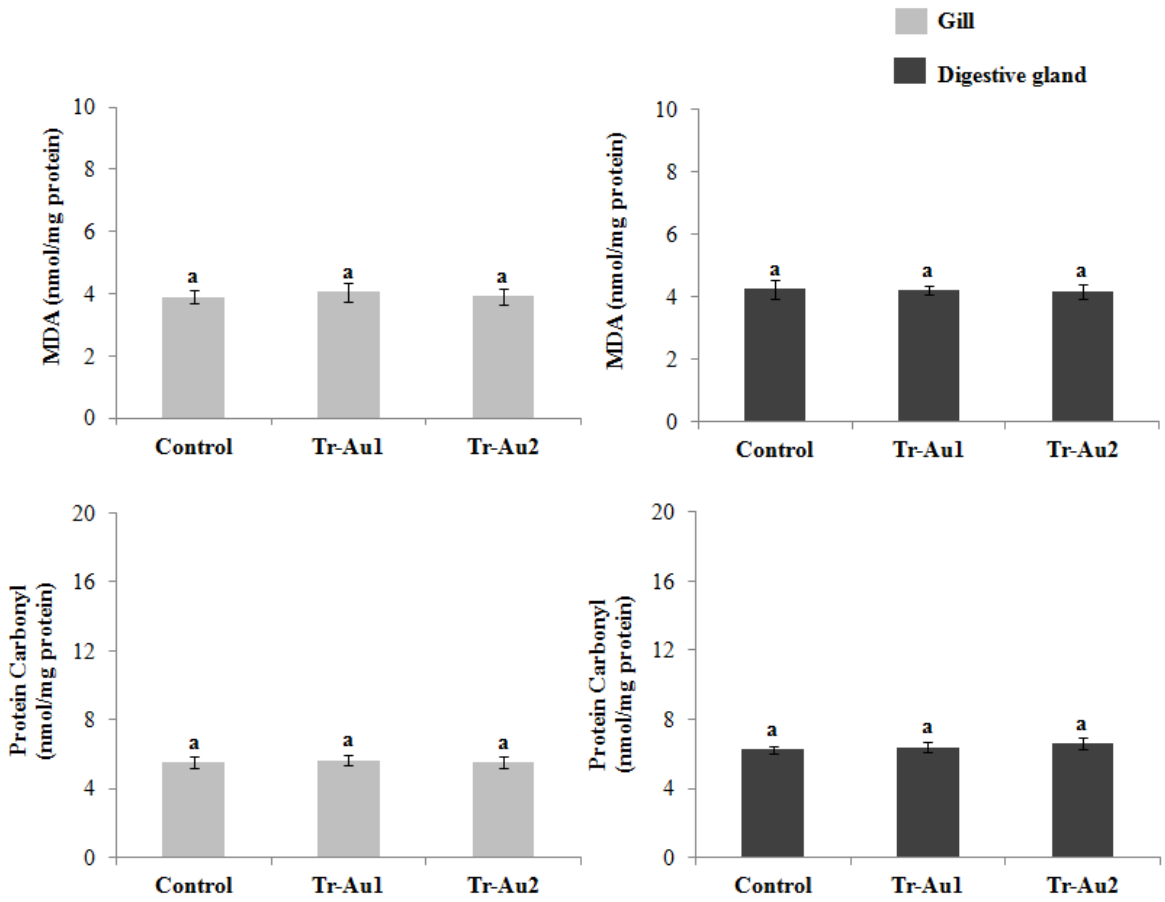

530

531 Fig. 5

532

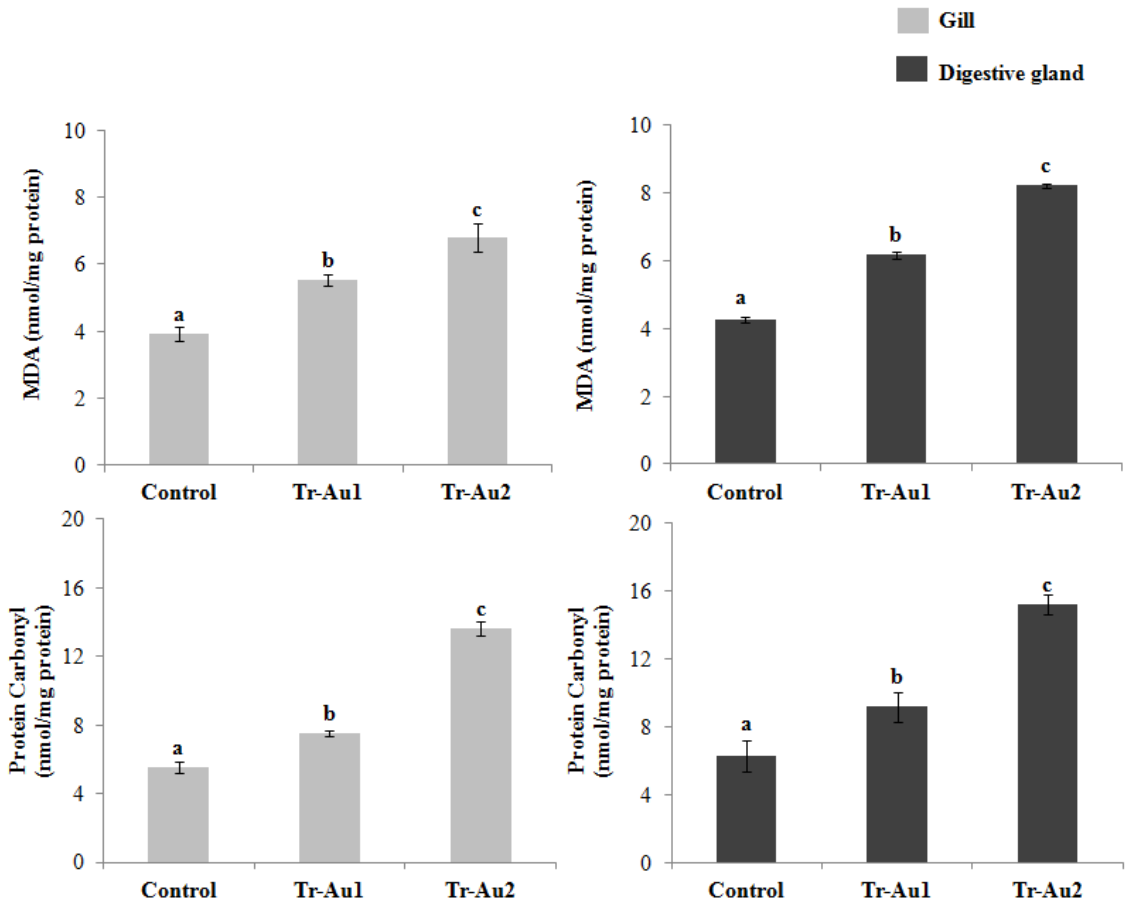
Gill
Digestive gland
MDA (nmol/mg protein)
Protein Carbonyl (nmol/mg protein)
Control
Tr-Au1
Tr-Au2
a
b
c

533

534 Fig. 6